Highly selective separation and resource recovery using forward osmosis membrane assembled by polyphenol network

Lu Elfa Peng [a], Zhikan Yao [b], Jixuan Chen [a], Hao Guo [a*], Chuyang Y. Tang [a*]

[a]Department of Civil Engineering, The University of Hong Kong, Pokfulam, Hong Kong SAR, China.

[b]College of Chemical and Biological Engineering, Zhejiang University, Hangzhou, 310027, China.

[*]Corresponding Authors:

Hao Guo, guohao7@hku.hk, +852 28578470

Chuyang Y. Tang, tangc@hku.hk, +852 28591976

Graphic abstract

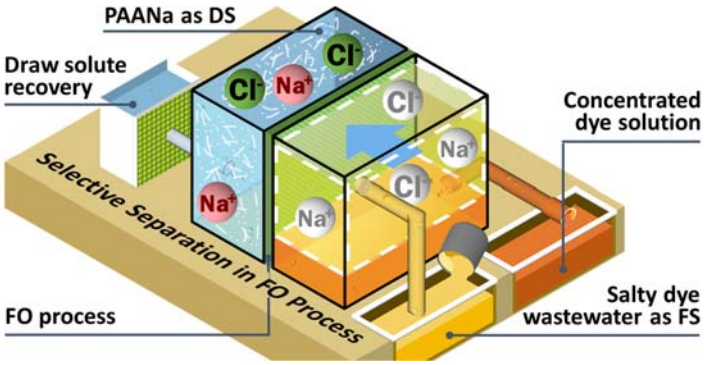

Abstract

We report a novel forward osmosis (FO) membrane prepared by a green tannic acid/iron (TA/Fe) coordination chemistry to selectively separate and recover organic source from salty water. The microscopic and x-ray photoelectron spectroscopy (XPS) characterization confirmed the formation of a thin continuous TA/Fe rejection layer with a thickness of 20~30 nm on a polyacrylonitrile (PAN) substrate. This TA/Fe-PAN membrane showed a high water permeability (A) of 14.2 ± 1.7 $Lm^{-2}h^{-1}bar^{-1}$, a high rejection of $99.5 \pm 0.1\%$ for a low-molecular dye sunset yellow and low rejection of $27.6 \pm 2.7\%$ for NaCl under reverse osmosis (RO) mode. The membrane selectivity to sunset yellow was nearly three orders of magnitude greater than that of NaCl, revealing its preference towards organic dye retention and salt passage. As a result of its higher water permeability and the prevention of salt accumulation during FO tests, the TA/Fe-PAN membrane showed significantly higher FO water flux compared to that of a commercially available polyamide thin film composite membrane. It could concentrate sunset yellow from a salty FS solution with a concentration ratio of 9.6 and mild salt accumulation at the water recovery ratio of 90%. The results demonstrated the feasibility of selective separation and resource recovery for target solutes from salty even more complicated water matrix via proper membrane chemistry design in FO.

Keywords:

Green membrane, tannic acid/iron complex, forward osmosis, selective separation, resource recovery.

1. Introduction

Forward osmosis (FO), an osmotically driven membrane process, has been considered as an alternative technology for water and wastewater treatment [1-3]. Unlike pressure-driven reverse osmosis (RO), FO enjoys several potential benefits such as low operating pressure and low fouling propensity [4-7]. Currently, the thin film composite (TFC) polyamide membranes are intensively used in FO [8-10] where the existing literature mainly emphasizes the critical importance of their high salt rejection (e.g., NaCl). However, such high salt rejection often comes at the expense of reduced water permeability as a result of their tradeoff relationship [11, 12]. In addition, high retention of salts from feed solution (FS) can lead to their accumulation in FS, resulting in reduced osmotic driving force and lower FO water flux [13-15].

Despite that salt rejection is a critical parameter for desalination-oriented applications, it is not necessarily important for FO processes used for non-desalination purposes. For instance, the pre-treatment of seawater desalination using FO should mainly focus on the retention of algae and scalants (e.g., calcium, sulfate) to minimize the risks of biofouling and scaling for RO process [7, 13, 16]. FO based urine treatment should target on high nutrients retention (e.g., nitrogen and phosphorous) to achieve resource recovery rather than simple salts removal [17]. In osmotically-driven membrane bioreactor (OMBR), high salt rejection would controversially deteriorate bioactivity which is unfavorable in the process [15, 18-20]. In these cases, high salt rejection (e.g., NaCl) is not the primary goal, contrarily, it can count against the FO separation efficiency because of severe salt accumulation. Presumably, an ideal FO membrane should be designed and optimized to fit in specific applications, where the valuable compounds can be selectively retained/recovered. For many resource recovery applications where salts are not the primary target, traditional polyamide membranes rooted from desalination applications may

not be suitable [21-23]. Therefore, it is worthwhile to develop alternative novel membrane materials to implement selective separation and resource recovery using FO process. Tannic acid/iron (TA/Fe) network has been reported as an effective and green rejection layer of nanofiltration membrane for the removal of micropollutants in water reuse [24, 25]. It enjoys several advantages including rapid formation and green fabrication process using low toxic chemicals [26, 27]. Nevertheless, there is no work to apply TA/Fe network for FO based applications.

In this study, a novel non-polyamide-based FO membrane using green tannic acid/iron (TA/Fe) coordination complex was explored to conduct selective separation and organic resource recovery from salty water using sunset yellow as a model organic solute. Systematic investigation of FO separation performance including water permeability, NaCl accumulation, and dye concentration were performed. The membrane selectivity towards dye/salt separation efficiency were analyzed and further compared with a polyamide-based FO membrane. The findings will expand the application range of FO-based separation process, especially for non-desalination purposes. It may inspire the design of novel FO membrane with highly-selective rejection of target solutes for specific applications.

2. Materials and methods

2.1. Chemicals

Unless specified otherwise, all solutions were prepared with deionized (DI) water supplied by a Milli-Q system (Millipore). Polyacrylonitrile (PAN, average molecular weight (MW) of ~150000, Sigma-Aldrich), dimethylformamide (DMF, ≥99.8%, Sigma-Aldrich), and lithium chloride anhydrous (LiCl, >98%, TCI) were used to prepare the PAN substrate. TA (General-Reagent) and iron chloride ($FeCl_3$, anhydrous, Dieckmann) were used to fabricate the green TA/Fe rejection layer. Poly(acrylic acid) (PAA, 50% in water, MW of ~3000, Aladdin) and sodium hydroxide (NaOH, Dieckmann) were used to prepare the draw solution (DS) of sodium polyacrylate (PAANa). Such draw solutes with large MW for FO applications have also been reported in the literature [28-31]. Sunset yellow (87%, Dieckmann) was selected as a model organic source in the FS. It is one of the commonly used water-soluble additives for food and pharmaceutical products such as beverages and bakery products [32-34]. Sodium chloride (NaCl, Uni-chem) was used to adjust solution chemistry. Polyethylene glycol (PEG, MW of ~400 and ~600, Aladdin), d-raffinose (99%, Macklin), sodium sulfate (Na_2SO_4, anhydrous, Uni-chem), calcium chloride ($CaCl_2$, Uni-chem) and 6-hydrate magnesium chloride ($MgCl_2 \cdot 6H_2O$, Uni-chem) were used to evaluate membrane separation properties under RO mode.

2.2. Membrane fabrication

The preparation of the PAN substrate has been reported in our previous work [35]. Briefly, a dope solution containing 18 wt% PAN and 2 wt% LiCl in DMF were spread into a film on a clean glass plate using an automatic film applicator (Elcometer 4340, Elcometer, gate height set at 150 μm). The casted film was coagulated in DI water at room temperature (~ 25 ˚C). The

nascent substrate was then rinsed and soaked with DI water before further using. The membrane selective layer was formed by coating a TA/Fe thin film with a TA/Fe molar ratio of 1:3 onto the PAN substrate [25, 26]. Specifically, the substrate was fixed in a custom-designed container only exposing its top surface in coating solution [36]. A 30 mL $FeCl_3$ solution (7.2 mM) was first added into the container for 30 s followed by adding equal volume of TA solution (2.4 mM) for 60 s to form the TA/Fe layer. The entire procedure was performed under moderate shaking at room temperature (~ 25 ˚C). The formed membrane (denoted as TA/Fe-PAN) was then thoroughly rinsed and soaked in DI water. A commercial polyamide thin film composite (TFC) FO membrane (HTI, Albany, OR) was used for comparison purpose.

2.3. Membrane characterization

Unless specified elsewhere, all membrane samples were vacuum-dried before characterization. A field-emission scanning electron microscopy (FE-SEM, S-4800, Hitachi, Japan) was used to scan membrane surface morphology at an acceleration voltage of 5.0 kV. The membrane samples were sputter-coated with a thin gold layer before SEM scanning. A transmission electron microscopy (TEM, Tecnai G^2 20 S-TWIN, FEI, USA) was used to characterize the cross-section structure of the membrane at an accelerating voltage of 100 kV. An x-ray photoelectron spectroscopy (XPS, Leybold, Sengyang, China) was used to analyze the elemental compositions of the membrane surface at 10 kV and 15 mA with a source of Al Kα gun (1496.3 eV). An electrokinetic analyzer (EKA, SurPASS 3, Anton Paar, Austria) was applied to investigate the zeta potential of membrane surface over a pH range of 3~9 in a background electrolyte solution of 1.0 mM KCl. The membrane samples were immersed in the background solution overnight before the zeta potential test.

2.4. RO separation performance

Membrane RO separation performance was evaluated using a laboratory-scale cross-flow filtration system (Appendix A) [37]. Each membrane coupon was installed in a cross-flow cell (CF042, Sterlitech, USA) with an effective area of 42 cm^2, and pre-compacted at 3 bar with a cross flow velocity of 22.4 cm/s for 2 h. DI water, 1 g/L salt solution (NaCl, Na_2SO_4, $CaCl_2$, or $MgCl_2$), 0.05 g/L sunset yellow solution or 0.2 g/L organic solute (PAA, PEG, or D-Raffinose) were used as the feed independently to evaluate membrane separation performance. Salt concentration was measured by a conductivity meter (Ultrameter II, Myron L Company, USA). Organic solute concentration was measured by a total organic carbon (TOC) analyzer (TOC-V CPH, Shimadzu, Japan). Sunset yellow concentration was measured by an UV/VIS spectrophotometer (UH5300, Hitachi, Japan). The detailed calculation of water permeability and the rejection of salts or solutes is attached in Appendix B.

2.5. FO separation performance

Membrane FO separation performance was evaluated using a laboratory-scale cross-flow FO filtration system (Fig. 1) [38]. Each membrane coupon was fixed in a cross-flow FO cell (CF042-FO, Sterlitech, USA) with an orientation of active layer facing the feed solution (AL-FS). Diamond-patterned spacers were placed on both sides of the membrane to provide support and improve mass transfer. The effective filtration area is 42 cm^2. Two gear pumps were used for the recirculation of FS and DS with the same flow rate of 11.7 cm/s for an experimental duration of 2 h. Water flux ($J_{v,FO}$) was obtained by weighing FS tank at a specific time interval using a balance connected to a data recording program. Reverse solute flux tests were performed with 1 L DI water as FS and 1 L PAANa solution over a concentration range (11.7 mM, 23.5 mM and 46.9 mM, whose osmotic pressure was approximately equivalent to 0.25

M, 0,5 M and 1 M NaCl, respectively) as DS [35]. The reverse solute flux (J_{ds}) was obtained as the slope of plotted $C_{d,fs}(V_{fs,0} - J_{v,FO}A_m t)/A_m$ versus t, where $C_{d,fs}$ (mM) is the draw solute concentration at time t (h) in FS, $V_{fs,0}$ (L) is the initial volume of FS, and A_m is the effective membrane area (m^2).

The dye/salt selective separation and dye recovery test was performed using 1 L FS containing 1 g NaCl and 0.05 g sunset yellow, and 1 L DS of 11.7 mM PAANa solution until achieving a water recovery ratio of 90% for FS. Samples from FS and DS were taken at the initial stage (i.e., water recovery 0%) and final stage (i.e., water recovery 90%). The concentration of chloride ion (Cl^-) was determined by ion chromatography (IC, LC 20AD, Shimadzu, Japan). At least 3 parallel experiments were conducted.

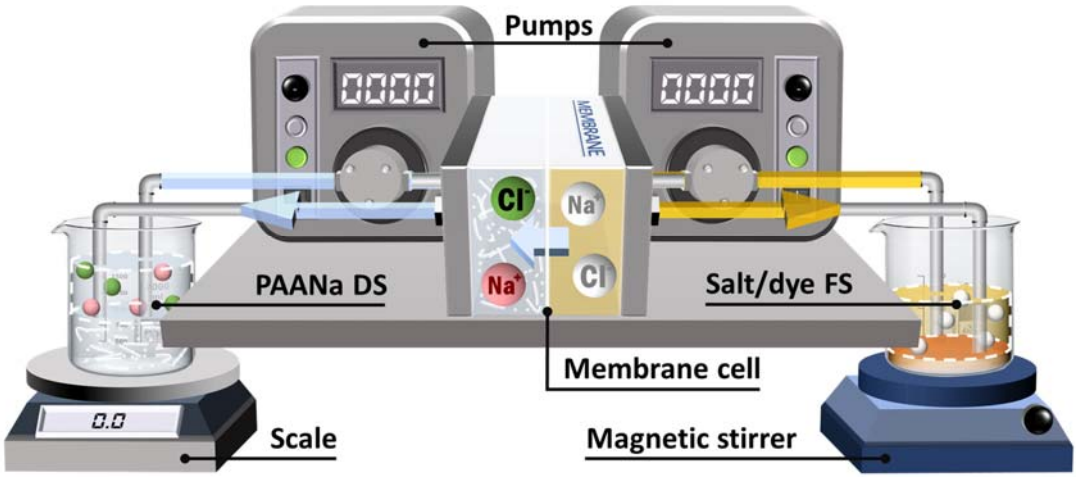

Fig. 1. Diagram of the laboratory-scale FO system.

3. Results and discussion

3.1. Membrane characterization

The virgin PAN substrate (Fig. 2A1) showed a smooth surface morphology in agreement with previous studies [39, 40]. No significant changes except some scattered particles were observed on the surface of TA/Fe-PAN membrane (Fig. 2A2). TEM micrographs gave a significant contrast of cross-section structure between the substrate and TA/Fe-PAN membrane. Compared to the virgin PAN substrate, the TA/Fe-PAN showed an additional continuous thin layer with a thickness of 20~30 nm on the top of the substrate (Fig. 2B2). The EDX elemental mapping showed a strong signal of Fe in the top thin layer (Appendix C). This result is consistent with previous studies that TA/Fe coordination complex could form a thin and continuous coating layer [24, 25].

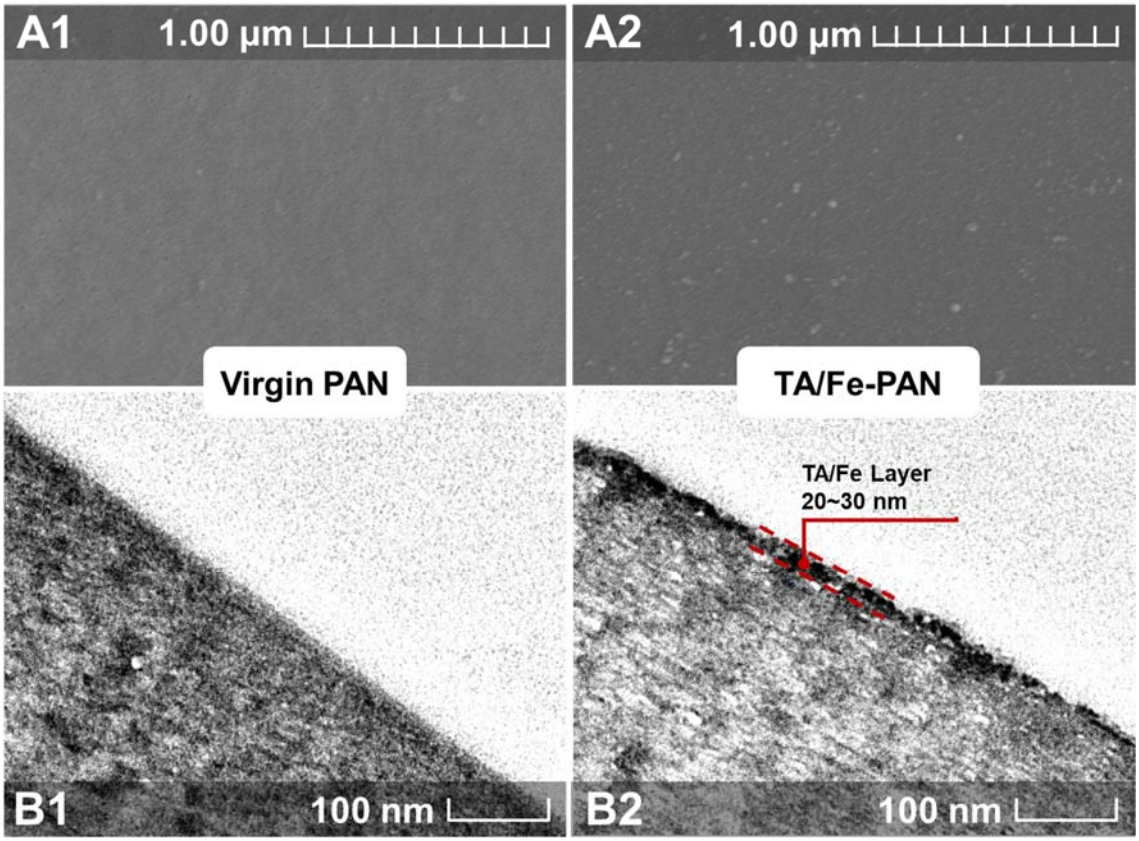

Fig. 2. Microscopic characterization of membranes. (A) SEM micrographs (top view), and (B) TEM micrographs (cross section) of the virgin PAN substrate (A1, B1) and the TA/Fe-PAN membrane (A2, B2).

XPS spectra confirmed the presence of Fe together with significantly increased signal of oxygen and reduced signal of nitrogen for TA/Fe-PAN (Fig. 3A), which gave strong evidence for the formation of TA/Fe coordination complex on the membrane surface. The detected C/O ratio of TA/Fe-PAN membrane was 2.3 which is close to the theoretical value of 1.7 for TA (Figure 3B), further implying the successful loading of TA/Fe layer on the PAN substrate. According to the existing literature, TA/Fe coating layer could be formed on various substrates thanks to the high affinity between TA molecules and the substrate [26, 41, 42]. In addition, our previous study also confirmed that the TA/Fe layer could maintain its integrity at low pH of 4 and had stable separation performance over a 10-day test [24], confirming the durability and stability of the layer.

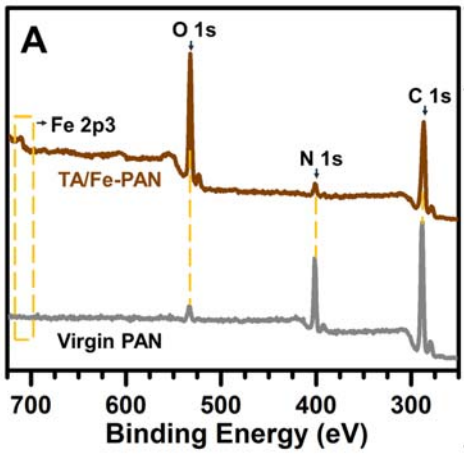

B

	Virgin PAN	TA/Fe-PAN
Fe2p3 (%)	Not detected	1.0
O 1s (%)	3.4	28.5
N 1s (%)	21.2	4.1
C 1s (%)	74.9	66.2
Detected C/O	22.2	2.3
Theoretical C/O	-	1.7
Detected C/N	3.5	16.2
Theoretical C/N	3	-

Fig. 3. (A) XPS spectra, (B) surface elemental contents, C/O and C/N ratios of the virgin PAN substrate and the TA/Fe-PAN membrane.

3.2. RO separation performance

Intrinsic separation properties of TA/Fe-PAN membrane including water permeability and solutes rejection were evaluated under RO mode (Table 1). The TA/Fe-PAN membrane had a water permeability (*A* value) of 14.2 ± 1.7 L m^{-2} h^{-1} bar^{-1} accompany with a rejection rate of 27.6 ± 2.7% for NaCl, which is significantly lower than that of HTI polyamide membrane (i.e., 88.4 ± 1.5 %) [35]. Meanwhile, it showed high rejections of sunset yellow (99.5 ± 0.1%) and PAANa (96.7 ± 1.1%). To reveal the underlying rejection mechanisms, the rejection of neutral compounds (i.e., PEG and raffinose) with similar molecular weight to sunset yellow were also investigated (Appendix E). The TA/Fe-PAN membrane showed relatively lower rejection of neutral compounds (75.9-83.1%) compared to charged compounds. The high rejection of dye could be attributed to the effect of size exclusion together with the effect of electrostatic repulsion thanks to the negatively charged membrane surface (Appendix D). The permeability of sunset yellow (i.e., B_{sun} of 0.2 ± 0.03 $Lm^{-2}h^{-1}$) was almost four order of magnitude lower than that of NaCl (i.e., B_{NaCl} of 109.8 ± 28.3 $Lm^{-2}h^{-1}$), revealing the great resistance to the organic dye for TA/Fe-PAN membrane. Furthermore, the membrane selectivity (i.e., *A/B*) to dye was nearly three orders of magnitude greater than that of NaCl, which facilitate its selective recovery of dye from salty solutions (Section 3.4).

Table 1. Separation performance of TA/Fe-PAN and HTI membrane for organic solutes and inorganic salts in RO.

Membrane	Solutes	Rejection (%)	Solute permeability *B* ($Lm^{-2}h^{-1}$)	Water permeability *A* ($Lm^{-2}h^{-1}bar^{-1}$)	Selectivity *A/B* (bar^{-1})
TA/Fe-PAN	PAANa	96.7 ± 1.1	1.2 ± 0.4	14.2 ± 1.7	12.8 ± 4.6
	Sunset Yellow	99.5 ± 0.1	0.2 ± 0.03		80.6 ± 13.6
	NaCl	27.6 ± 2.7	109.8 ± 28.3		0.1 ± 0.04
HTI[a]	NaCl	88.4 ± 1.5	0.2 ± 0.05	2.1 ± 0.3	12.5 ± 1.8

a. The separation performance of HTI for NaCl was from the previous work [35].

3.3. FO separation performance

The FO performance of TA/Fe-PAN including water flux and reverse solute flux using different DS concentrations were systematically tested. Reasonably high FO water flux was obtained at a relatively low DS concentration of 11.7 mM (e.g., 13.1 $Lm^{-2}h^{-1}$ when using 1 g/L NaCl as the FS). The water flux of TA/Fe-PAN for both two FS (i.e., DI water and 1g/L NaCl solution) were only marginally increased with increasing DS concentration to 46.9 mM, which is attributed to severe internal concentration polarization [30, 43]. The reverse flux of PAANa was mild (< 0.1 $mMm^{-2}h^{-1}$ in all cases) due to its low solute permeability (Table 1).

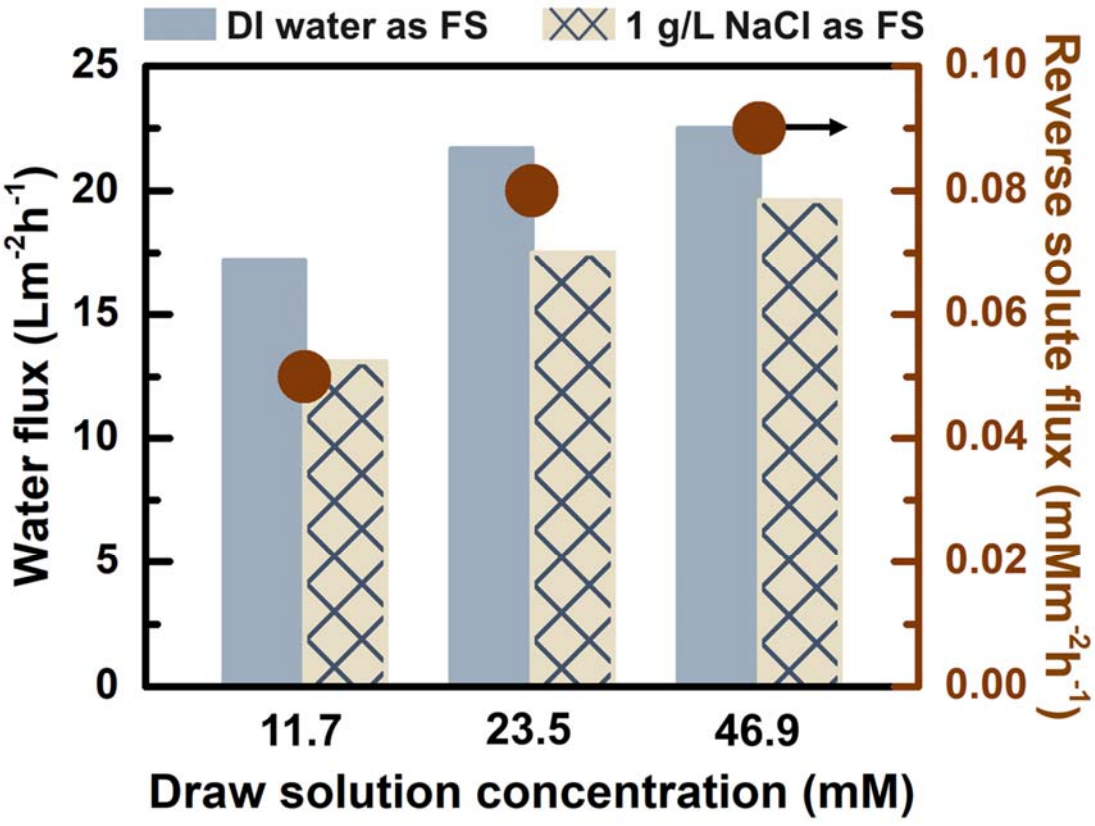

Fig. 4. Effects of different DS concentration on water flux and reverse solute flux of TA/Fe-PAN membrane. Testing conditions: experiments were conducted using DI water or 1 g/L NaCl as FS and PAANa solution (11.7, 23.5, or 46.9 mM) as DS at AL-FS mode for 2 h.

Compared to traditional polyamide based membrane (e.g., HTI TFC membrane), TA/Fe-PAN harvested over 5 times higher water flux using the same DS concentration (46.9 mM), which can be attributed to its higher water permeability (14.2 ± 1.7 $Lm^{-2}h^{-1}bar^{-1}$) than HTI (2.1 $Lm^{-2}h^{-1}bar^{-1}$) [35]. Meanwhile, TA/Fe-PAN presents much lower propensity of salt accumulation comparing to that of HTI because of its higher NaCl permeability. Lower salt accumulation is beneficial in maintaining the transmembrane osmotic driving force and therefore a higher FO water flux. In contrast, high salt accumulation can significantly reduce the driving force, resulting in greatly dropped water flux [44]. Although HTI membrane presented a similar even higher rejection of different organic solutes compared to the TA/Fe-PAN membrane (Appendix E), the high salt rejection may significantly restrict its selective separation efficiency and water production.

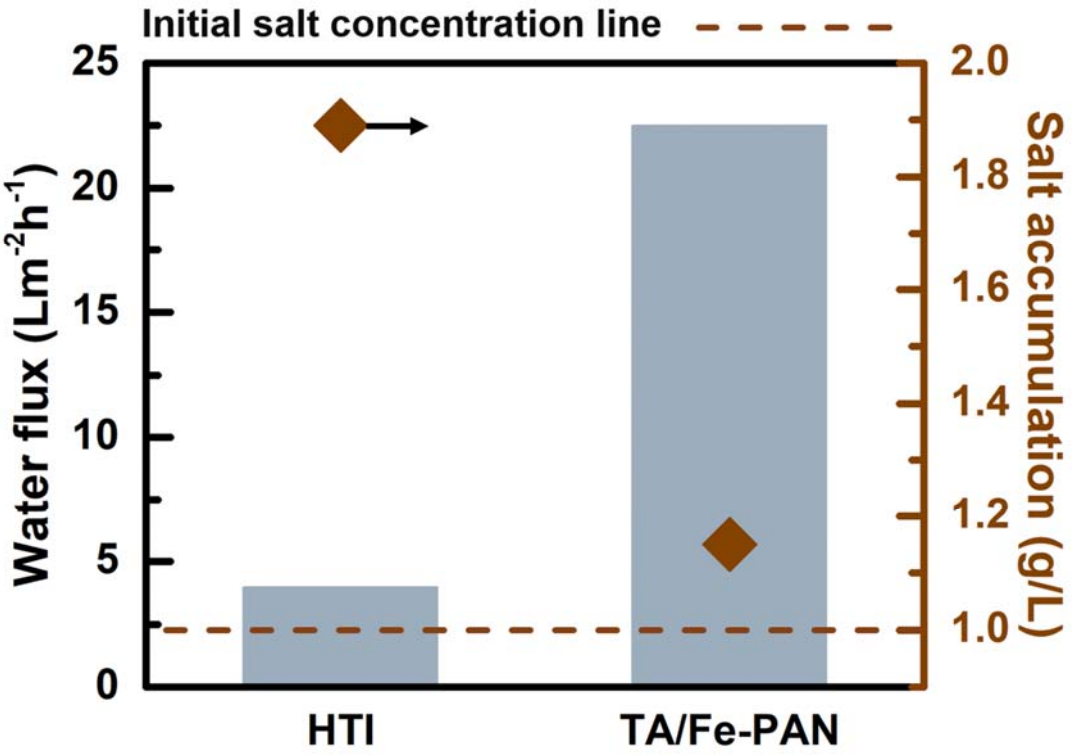

Fig. 5. Water flux and salt accumulation of membranes HTI and TA/Fe-PAN. Testing conditions: All tests were performed at AL-FS mode. Water flux was evaluated using 46.9 mM PAANa solution and pure water as DS and FS, respectively. Salt accumulation was tested using 1 g/L NaCl as FS, separately using 46.9 mM M PAANa as DS for HTI and 4.7 mM PAANa as DS for TA/Fe-PAN to get similar initial water flux. The salt accumulation degree was evaluated by measuring the NaCl concentration in FS at the water recovery ratio of 50%.

3.4. Selective separation and dye recovery in FO

Fig. 6 presents the results of selectively separating and recovering dye from a salty solution using TA/Fe-PAN FO membrane. At a water recovery ratio of 90%, sunset yellow was concentrated from 0.05 to 0.48 g/L (Fig. 6A). Further analysis indicates that sunset yellow gave a concentration ratio of 9.6 (significant color contrast between initial and concentrated solutions) (Fig. 6B), which was in good agreement with the volumetric concentration factor of

10. In contrast, NaCl was only concentrated from 1.0 g/L to 1.6 g/L, corresponding to a concentration ratio of merely 1.6 and thus a mild salt accumulation in FS. The significantly different concentration behavior between sunset yellow and NaCl can be attributed to the membrane selectivity to different solutes (Table 1), where TA/Fe-PAN membrane preferentially retains the dye and let NaCl passing through. In addition, TA/Fe layer also showed an antifouling property during long-term running [25, 45, 46].The results demonstrate the feasibility of selective separation of targeted organic solutes (e.g., dye) from salty water to further achieve resource recovery by properly designed membrane chemistry.

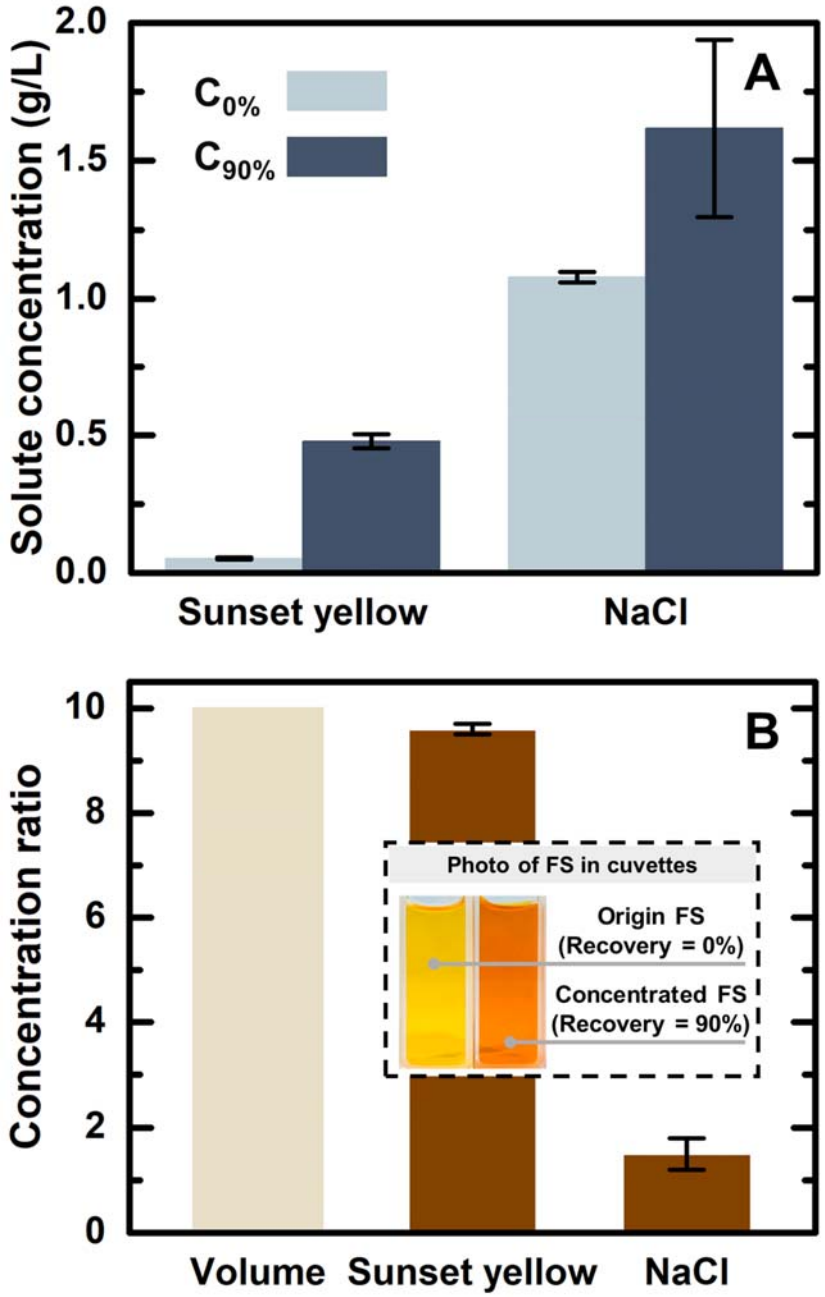

Fig. 6. The performance of selective separation and dye concentration in FO by TA/Fe-PAN membrane. (A) The initial and final concentration of sunset yellow and NaCl, where $C_{0\%}$ is the initiate concentration of solute in FS (0% recovery), $C_{90\%}$ is the final concentration of solute in FS (90% recovery). (B) Solute concentration ratio is the ratio of $C_{90\%}$/ $C_{0\%}$ for sunset yellow or NaCl at the water recovery of 90% (i.e., FS volume was concentrated by 10 times). Testing conditions: 11.7 mM PAANa was applied as DS, the mixing solution of 0.05 g/L sunset yellow and 1g/L NaCl was prepared as FS.

4. Conclusions

In this study, we reported a green FO membrane using TA/Fe coordination complex to perform selective separation and organic dye recovery from a salty water. The resulted TA/Fe-PAN membrane had a thin rejection layer of 20-30 nm, who showed a much higher water permeability than that of a polyamide based TFC membrane (i.e., HTI membrane). It had a superior rejection of sunset yellow (99.5 ± 0.1%) and a low rejection of NaCl (27.6 ± 2.7%), resulting in the membrane selectivity to sunset yellow dye (i.e., A/B_{sun}) which was three orders of magnitude greater than its selectivity to NaCl (i.e., A/B_{NaCl}). The great selectivity allowed the membrane to recover the target (e.g., sunset yellow) from a salty FS solution with a concentration ratio of 9.6 (very close to the ideal ratio of 10 for completed concentration) at the water recovery ratio of 90%. Meanwhile, NaCl could passed the membrane more easily, resulting in low salt accumulation in the FS side which could retard the drop of osmotic pressure difference across the membrane (thus suspend the reduction of FO water flux).

In existing literature, FO membranes are often designed and evaluated by the rejection of salts [3, 47]. However, salts are not always the primary targets in some specific applications such as food concentration [48] and resource recovery in wastewater [49, 50]. Actually, allowing selective passage of salts can effectively mitigate its accumulation, a critical challenge preventing high water recovery in many FO applications [50, 51]. The findings in the current study demonstrate the possibility of highly selective separation for target source from a salty water with properly designed membrane chemistry. Based on the results, the novel TA/Fe-PAN FO membrane can be potentially used for the wastewater decoloring and dye recovery from a salty wastewater in textile industries [51-53]. It may also be used for the selective separation of scaling precursors (e.g., SO_4^{2-}) and organic foulants in the pre-treatment of seawater and brackish water [35, 54, 55].

Acknowledgments

We thank the State Key Laboratory of Separation Membranes and Membranes Processes of Tianjin Polytechnic University (No.M3-201701) for providing XPS analysis. Ms. Vicky Fung is thanked for the IC test. We also appreciate the Electro Microscopic Unit (EMU) at The University of Hong Kong for SEM and TEM characterization.

Appendix A. Laboratory-scale RO system

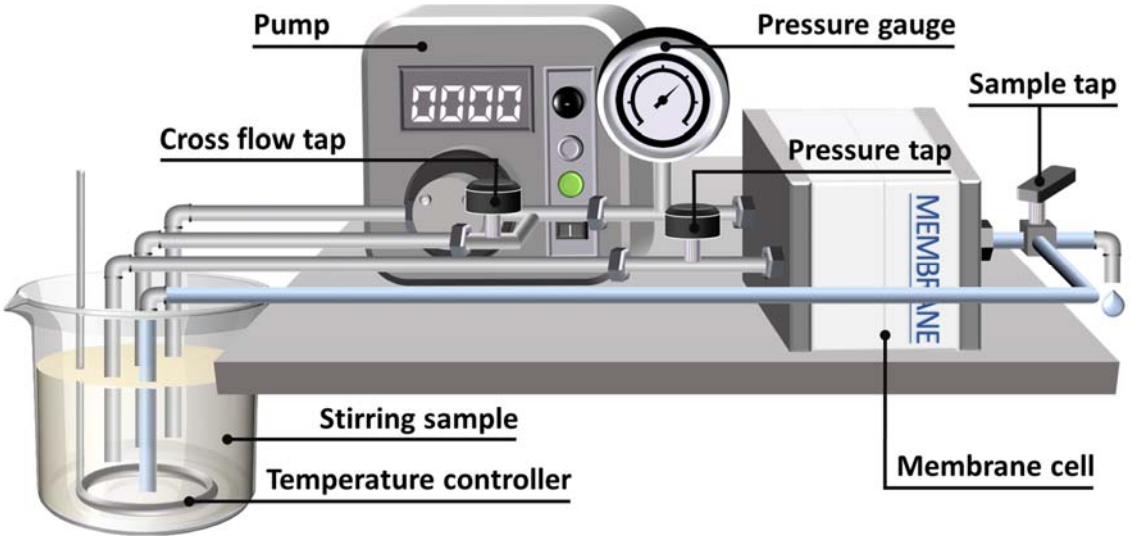

Fig. A1. Diagram of the laboratory-scale RO system.

Fig. A1 shows the cross-flow laboratory-scale RO system used in this work, where the membrane was tested in a cross-flow cell (effective filtration area of 42 cm^2) with a cross flow velocity of 22.4 cm/s at 3 bar under 25 ˚C.

Appendix B. Calculation of membrane separation properties

In RO mode, the water flux, $J_{v,RO}$ ($Lm^{-2}h^{-1}$), was calculated via measuring the mass of the collected permeate, Δm (kg), over a specific time interval, Δt (h), according to the following Eq. (B1):

$$J_{v,RO} = \frac{\Delta m}{\Delta t \times a \times \rho} \quad \text{(B1)}$$

where a (m^2) is the effective membrane area and ρ is density of water. The pure water permeability coefficient, A ($Lm^{-2}h^{-1}bar^{-1}$), was calculated from Eq. (B2) using DI water as the feed solution:

$$A = \frac{J_{v,RO}}{\Delta P - \Delta \pi} \quad \text{(B2)}$$

where ΔP (bar) is the hydraulic pressure difference across the membrane, $\Delta \pi$ (bar) is the osmotic pressure difference across the membrane. Membrane rejection (R_{RO}) to dye or salts were calculated by Eq. (B3):

$$R_{RO} = \frac{C_f - C_p}{C_f} \times 100\% \quad \text{(B3)}$$

where C_f and C_p are the concentration of the feed and the permeate, respectively. Dye concentration was measured using an UV/VIS spectrophotometer, and salt concentration was determined by a portable conductivity meter (Ultrameter II, Myron L), which can be subsequently converted to concentration [56]. The solute permeability coefficient (B) was calculated from Eq. (B4):

$$B = (\frac{1}{R_{RO}} - 1) \times J_{v,RO} \quad \text{(B4)}$$

In FO-mode, membrane rejection (R_{FO}) was defined as Eq. (B5) [57]:

$$R_{FO} = 1 - \frac{J_s}{J_{v,FO} C_{fs}} \times 100\% \quad \text{(B5)}$$

where J_s ($gm^{-2}h^{-1}$) is the reverse solute flux obtained as the slope of plotted $C_{fs,t}(V_{fs,0} - J_{v,FO}A_m t)/A_m$ versus t, where $C_{fs,t}$ (mM) is the solute concentration at time t (h) in FS, $V_{fs,0}$ (L) is the initial volume of FS, and A_m is the effective membrane area (m^2). $J_{v,FO}$ ($Lm^{-2}h^{-1}$) is water flux in FO, C_{fs} (g/L) is the solute concentration in FS.

Appendix C. TEM cross-section image and EDX mapping

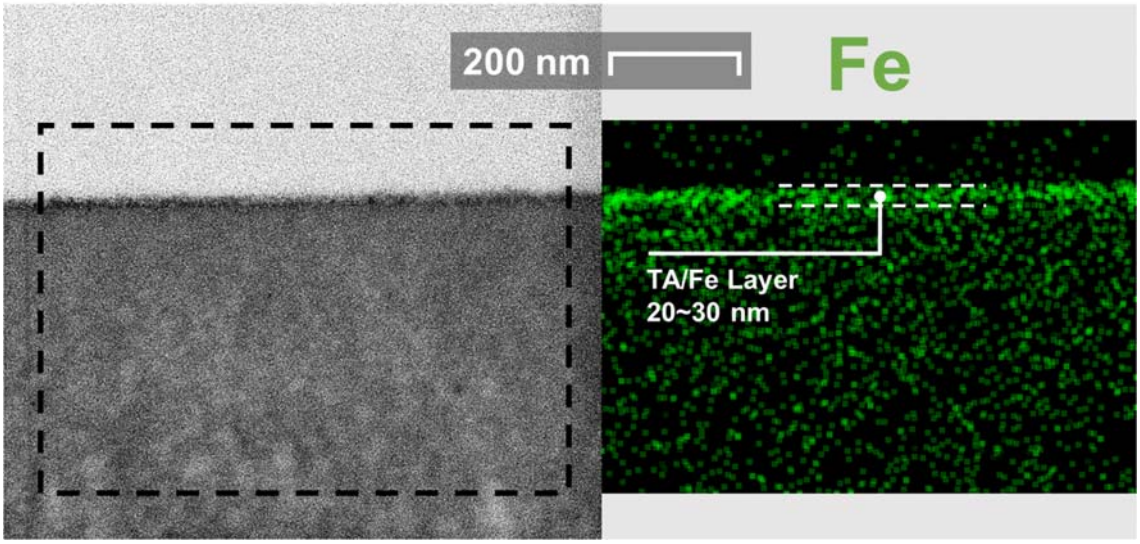

Fig. C1. TEM cross-section image and EDX elemental mapping of iron (Fe) for the TA/Fe-PAN membrane.

The EDX mapping confirmed the presence of Fe in the top thin layer, indicating the successful formation of TA/Fe complex rejection layer.

Appendix D. Zeta potential results of membranes

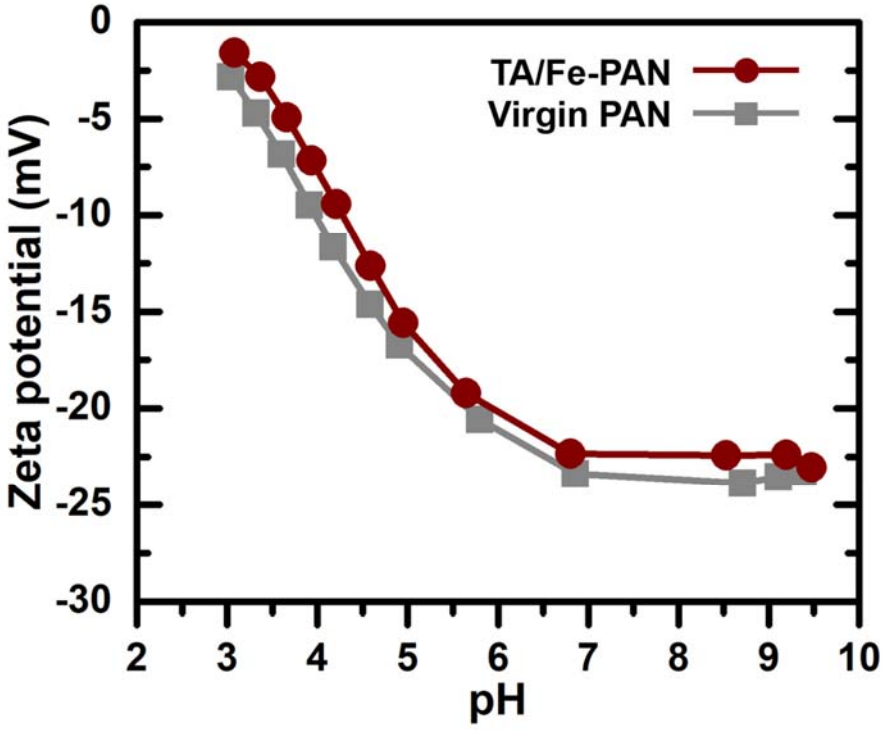

Fig. D1. Zeta potential of the virgin PAN membrane and the TA/Fe-PAN membrane.

Fig. D1 shows no obvious difference on the surface zeta potential between TA/Fe-PAN and virgin PAN.

Appendix E. Membrane separation performance in RO mode

Table. E1. TA/Fe-PAN membrane separation performance of organic solutes and inorganic salts.

Membrane	Solutes	Molecular weight	Rejection (%)	Solute permeability B ($Lm^{-2}h^{-1}$)	A/B (bar^{-1})
HTI[a]	Glucose	180	94%	-	
	PAANa	~3400	> 99%		
TA/Fe-PAN			96.7 ± 1.1	1.2 ± 0.4	12.8 ± 4.6
	PEG	600	83.1	8.7	1.6
	D-Raffinose	504	79.5	11.0	1.3
	Sunset yellow	452	99.5 ± 0.1	0.2 ± 0.03	80.6 ± 13.6
	PEG	400	75.9	13.5	1.1
	Na_2SO_4	142	87.6 ± 0.3	5.3 ± 0.4	2.7 ± 0.2
	$CaCl_2$	111	17.0 ± 0.7	207.0 ± 23.9	0.1 ± 0.01
	$MgCl_2$	95	18.9 ± 1.5	167.7 ± 17.3	0.1 ± 0.01
	NaCl	58	27.6 ± 2.7	109.8 ± 28.3	0.1 ± 0.04

Note:

a. The data of HTI membrane rejection to organic solutes are adopted from literature [35].

Table E1 listed the rejection rates of various organic solutes and inorganic salts by the TA/Fe-PAN membrane. The rejection of organic solutes with molecular weight (MW) of 400 to 600 were 75.9% to 99.5%, which was lower than the rejection of sunset yellow (MW=452). The higher rejection of sunset yellow could be attributed to the combined effects of size exclusion and charge repulsion. The rejection of Na_2SO_4 (87.6%) was much higher than the rejection of $CaCl_2$ (17.0%) and $MgCl_2$ (18.9%), suggesting the important role of electrostatic repulsion between anions (e.g., SO_4^{2-}) and the negatively charged membrane surface.

Appendix F. Concentration of sunset yellow and NaCl in different experimental conditions

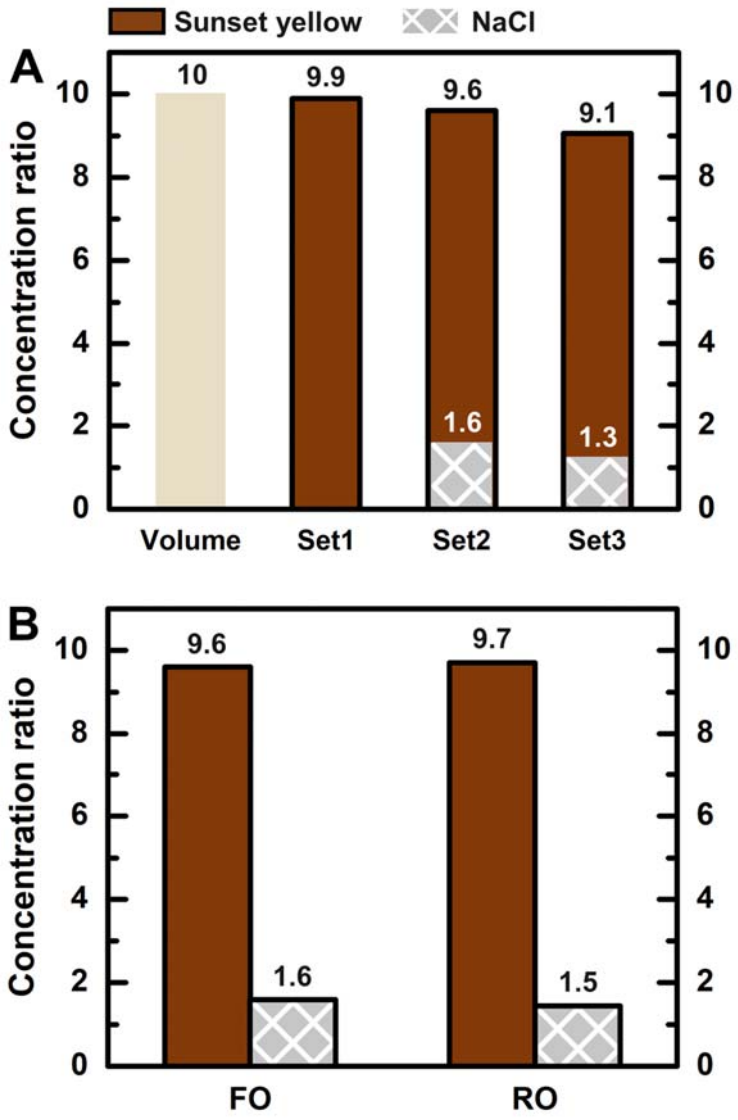

Fig. F1. (A) Concentration ratio ($C_{90\%}$/ $C_{0\%}$) of sunset yellow and NaCl in FO using different FS and (B) comparison of concentration behavior under FO and RO mode at water recovery ratio of 90%. Experimental conditions: (A) 11.7 mM PAANa was applied as DS. The FS used in Set1, 2, and 3 were 0.05g/L sunset yellow, 0.05g/L sunset yellow mixed with 1g/L NaCl, and 0.5g/L sunset yellow mixed with 1g/L NaCl respectively. (B) FO experimental conditions was same with Set2. RO experiment was conducted using 0.05g/L sunset yellow and 1g/L NaCl as feed solution at 3 bar.

372

373 Fig. F1A showed concentration ratios of sunset yellow and NaCl in FO using different FS. In
374 the experiment using FS of pure dye solution without NaCl (set1), the dye concentration ratio
375 was 9.9, which was slightly higher than the ratio of 9.6 from the case using an FS of dye/NaCl
376 mixture. These results indicate that NaCl enrichment had mild effect on the separation and
377 concentration of dye. There was no significant difference for the concentration performance
378 between FO and RO (Fig. F1B).

References

[1] T. Cath, A. Childress, M. Elimelech, Forward osmosis: Principles, applications, and recent developments, J. Membr. Sci., 281 (2006) 70-87.

[2] T.-S. Chung, S. Zhang, K.Y. Wang, J. Su, M.M. Ling, Forward osmosis processes: Yesterday, today and tomorrow, Desalination, 287 (2012) 78-81.

[3] N. Akther, A. Sodiq, A. Giwa, S. Daer, H.A. Arafat, S.W. Hasan, Recent advancements in forward osmosis desalination: A review, Chem. Eng. J., 281 (2015) 502-522.

[4] S. Lee, C. Boo, M. Elimelech, S. Hong, Comparison of fouling behavior in forward osmosis (FO) and reverse osmosis (RO), J. Membr. Sci., 365 (2010) 34-39.

[5] S. Zhao, L. Zou, C.Y. Tang, D. Mulcahy, Recent developments in forward osmosis: Opportunities and challenges, J. Membr. Sci., 396 (2012) 1-21.

[6] K. Lutchmiah, A.R. Verliefde, K. Roest, L.C. Rietveld, E.R. Cornelissen, Forward osmosis for application in wastewater treatment: a review, Water Res., 58 (2014) 179-197.

[7] Q. She, R. Wang, A.G. Fane, C.Y. Tang, Membrane fouling in osmotically driven membrane processes: A review, J. Membr. Sci., 499 (2016) 201-233.

[8] N.Y. Yip, A. Tiraferri, W.A. Phillip, J.D. Schiffman, M. Elimelech, High performance thin-film composite forward osmosis membrane, Environ. Sci. Technol., 44 (2010) 3812-3818.

[9] A. Tiraferri, N.Y. Yip, W.A. Phillip, J.D. Schiffman, M. Elimelech, Relating performance of thin-film composite forward osmosis membranes to support layer formation and structure, J. Membr. Sci., 367 (2011) 340-352.

[10] N. Ma, J. Wei, R. Liao, C.Y. Tang, Zeolite-polyamide thin film nanocomposite membranes: Towards enhanced performance for forward osmosis, J. Membr. Sci., 405-406 (2012) 149-157.

[11] H.B. Park, J. Kamcev, L.M. Robeson, M. Elimelech, B.D. Freeman, Maximizing the right stuff: The trade-off between membrane permeability and selectivity, Science, 356 (2017) eaab0530.

[12] Z. Yang, H. Guo, C.Y. Tang, The upper bound of thin-film composite (TFC) polyamide membranes for desalination, J. Membr. Sci., 590 (2019).

[13] A. Achilli, T.Y. Cath, E.A. Marchand, A.E. Childress, The forward osmosis membrane bioreactor: A low fouling alternative to MBR processes, Desalination, 239 (2009) 10-21.

[14] W.C.L. Lay, Q. Zhang, J. Zhang, D. McDougald, C. Tang, R. Wang, Y. Liu, A.G. Fane, Study of integration of forward osmosis and biological process: Membrane performance under elevated salt environment, Desalination, 283 (2011) 123-130.

[15] D. Xiao, C.Y. Tang, J. Zhang, W.C.L. Lay, R. Wang, A.G. Fane, Modeling salt accumulation in osmotic membrane bioreactors: Implications for FO membrane selection and system operation, J. Membr. Sci., 366 (2011) 314-324.

[16] J. Zhang, W.L.C. Loong, S. Chou, C. Tang, R. Wang, A.G. Fane, Membrane biofouling and scaling in forward osmosis membrane bioreactor, J. Membr. Sci., 403-404 (2012) 8-14.

[17] J. Zhang, Q. She, V.W. Chang, C.Y. Tang, R.D. Webster, Mining nutrients (N, K, P) from urban source-separated urine by forward osmosis dewatering, Environ. Sci. Technol., 48 (2014) 3386-3394.

[18] M.S. Moussa, D.U. Sumanasekera, S.H. Ibrahim, H.J. Lubberding, C.M. Hooijmans, H.J. Gijzen, M.C. van Loosdrecht, Long term effects of salt on activity, population structure and floc characteristics in enriched bacterial cultures of nitrifiers, Water Res., 40 (2006) 1377-1388.

[19] W.C. Lay, Y. Liu, A.G. Fane, Impacts of salinity on the performance of high retention membrane bioreactors for water reclamation: A review, Water Res., 44 (2010) 21-40.

[20] G. Qiu, Y.P. Ting, Osmotic membrane bioreactor for wastewater treatment and the effect of salt accumulation on system performance and microbial community dynamics, Bioresour. Technol., 150 (2013) 287-297.

[21] D. Li, H.T. Wang, Recent developments in reverse osmosis desalination membranes, J. Mater. Chem., 20 (2010) 4551-4566.

[22] K.P. Lee, T.C. Arnot, D. Mattia, A review of reverse osmosis membrane materials for desalination—Development to date and future potential, J. Membr. Sci., 370 (2011) 1-22.

[23] C.Y. Tang, Z. Yang, H. Guo, J.J. Wen, L.D. Nghiem, E. Cornelissen, Potable Water Reuse through Advanced Membrane Technology, Environ. Sci. Technol., 52 (2018) 10215-10223.

[24] H. Guo, Z. Yao, Z. Yang, X. Ma, J. Wang, C.Y. Tang, A One-Step Rapid Assembly of Thin Film Coating Using Green Coordination Complexes for Enhanced Removal of Trace Organic Contaminants by Membranes, Environ. Sci. Technol., 51 (2017) 12638-12643.

[25] H. Guo, L.E. Peng, Z.K. Yao, Z. Yang, X.H. Ma, C.Y.Y. Tang, Non-Polyamide Based Nanofiltration Membranes Using Green Metal-Organic Coordination Complexes: Implications for the Removal of Trace Organic Contaminants, Environ. Sci. Technol., 53 (2019) 2688-2694.

[26] H. Ejima, J.J. Richardson, K. Liang, J.P. Best, M.P. van Koeverden, G.K. Such, J. Cui, F. Caruso, One-step assembly of coordination complexes for versatile film and particle engineering, Science, 341 (2013) 154-157.

[27] L.Q. Xu, K.-G. Neoh, E.-T. Kang, Natural polyphenols as versatile platforms for material engineering and surface functionalization, Prog. Polym. Sci., 87 (2018) 165-196.

[28] R. Wei, S. Zhang, Y. Cui, R.C. Ong, T.-S. Chung, B.J. Helmer, J.S. de Wit, Highly permeable forward osmosis (FO) membranes for high osmotic pressure but viscous draw solutes, J. Membr. Sci., 496 (2015) 132-141.

[29] Q. Ge, T.S. Chung, Oxalic acid complexes: promising draw solutes for forward osmosis (FO) in protein enrichment, Chem Commun (Camb), 51 (2015) 4854-4857.

[30] S. Qi, Y. Li, Y. Zhao, W. Li, C.Y. Tang, Highly efficient forward osmosis based on porous membranes--applications and implications, Environ. Sci. Technol., 49 (2015) 4690-4695.

[31] Q. Ge, G. Han, T.S. Chung, Effective As(III) Removal by A Multi-Charged Hydroacid Complex Draw Solute Facilitated Forward Osmosis-Membrane Distillation (FO-MD) Processes, Environ. Sci. Technol., 50 (2016) 2363-2370.

[32] M. Sardi, Y. Haldemann, H. Nordmann, B. Bottex, B. Safford, B. Smith, D. Tennant, J. Howlett, P.R. Jasti, Use of retailer fidelity card schemes in the assessment of food additive intake: Sunset Yellow a case study, Food Addit Contam Part A Chem Anal Control Expo Risk Assess, 27 (2010) 1507-1515.

[33] K. Rovina, P.P. Prabakaran, S. Siddiquee, S.M. Shaarani, Methods for the analysis of Sunset Yellow FCF (E110) in food and beverage products- a review, TrAC, Trends Anal. Chem., 85 (2016) 47-56.

[34] S. Lehto, M. Buchweitz, A. Klimm, R. Strassburger, C. Bechtold, F. Ulberth, Comparison of food colour regulations in the EU and the US: a review of current provisions, Food Addit Contam Part A Chem Anal Control Expo Risk Assess, 34 (2017) 335-355.

[35] Z. Yao, L.E. Peng, H. Guo, W. Qing, Y. Mei, C.Y. Tang, Seawater pretreatment with an NF-like forward osmotic membrane: Membrane preparation, characterization and performance comparison with RO-like membranes, Desalination, 470 (2019).

[36] H. Guo, Y. Deng, Z. Tao, Z. Yao, J. Wang, C. Lin, T. Zhang, B. Zhu, C.Y. Tang, Does Hydrophilic Polydopamine Coating Enhance Membrane Rejection of Hydrophobic Endocrine-Disrupting Compounds?, Environ. Sci. Technol. Lett., 3 (2016) 332-338.

[37] Z. Yao, H. Guo, Z. Yang, C. Lin, B. Zhu, Y. Dong, C.Y. Tang, Reactable substrate participating interfacial polymerization for thin film composite membranes with enhanced salt rejection performance, Desalination, 436 (2018) 1-7.

[38] H. Guo, Z. Yao, J. Wang, Z. Yang, X. Ma, C.Y. Tang, Polydopamine coating on a thin film composite forward osmosis membrane for enhanced mass transport and antifouling performance, J. Membr. Sci., 551 (2018) 234-242.

[39] C. Qiu, S. Qi, C.Y. Tang, Synthesis of high flux forward osmosis membranes by chemically crosslinked layer-by-layer polyelectrolytes, J. Membr. Sci., 381 (2011) 74-80.

[40] S. Qi, C.Q. Qiu, Y. Zhao, C.Y. Tang, Double-skinned forward osmosis membranes based on layer-by-layer assembly—FO performance and fouling behavior, J. Membr. Sci., 405-406 (2012) 20-29.

[41] J. Borges, J.F. Mano, Molecular interactions driving the layer-by-layer assembly of multilayers, Chem. Rev., 114 (2014) 8883-8942.

[42] F. Reitzer, M. Allais, V. Ball, F. Meyer, Polyphenols at interfaces, Adv. Colloid Interface Sci., 257 (2018) 31-41.

[43] C.Y. Tang, Q. She, W.C.L. Lay, R. Wang, A.G. Fane, Coupled effects of internal concentration polarization and fouling on flux behavior of forward osmosis membranes during humic acid filtration, J. Membr. Sci., 354 (2010) 123-133.

[44] W.C.L. Lay, J. Zhang, C. Tang, R. Wang, Y. Liu, A.G. Fane, Factors affecting flux performance of forward osmosis systems, J. Membr. Sci., 394-395 (2012) 151-168.

[45] S. Kim, T. Gim, S.M. Kang, Versatile, tannic acid-mediated surface PEGylation for marine antifouling applications, ACS Appl Mater Interfaces, 7 (2015) 6412-6416.

[46] M. Li, L. Wu, C. Zhang, W. Chen, C. Liu, Hydrophilic and antifouling modification of PVDF membranes by one-step assembly of tannic acid and polyvinylpyrrolidone, Appl. Surf. Sci., 483 (2019) 967-978.

[47] R. Valladares Linares, Z. Li, S. Sarp, S.S. Bucs, G. Amy, J.S. Vrouwenvelder, Forward osmosis niches in seawater desalination and wastewater reuse, Water Res., 66 (2014) 122-139.

[48] V. Sant'Anna, L.D.F. Marczak, I.C. Tessaro, Membrane concentration of liquid foods by forward osmosis: Process and quality view, J. Food Eng., 111 (2012) 483-489.

[49] M. Xie, L.D. Nghiem, W.E. Price, M. Elimelech, Toward Resource Recovery from Wastewater: Extraction of Phosphorus from Digested Sludge Using a Hybrid Forward Osmosis–Membrane Distillation Process, Environ. Sci. Technol. Lett., 1 (2014) 191-195.

[50] Y.-N. Wang, R. Wang, W. Li, C.Y. Tang, Whey recovery using forward osmosis – Evaluating the factors limiting the flux performance, J. Membr. Sci., 533 (2017) 179-189.

[51] M. Li, X. Wang, C.J. Porter, W. Cheng, X. Zhang, L. Wang, M. Elimelech, Concentration and Recovery of Dyes from Textile Wastewater Using a Self-Standing, Support-Free Forward Osmosis Membrane, Environ. Sci. Technol., 53 (2019) 3078-3086.

[52] J. Huang, K. Zhang, The high flux poly (m-phenylene isophthalamide) nanofiltration membrane for dye purification and desalination, Desalination, 282 (2011) 19-26.

[53] I. Petrinić, N. Bajraktari, C. Hélix-Nielsen, Membrane technologies for water treatment and reuse in the textile industry, in: Advances in Membrane Technologies for Water Treatment, 2015, pp. 537-550.

[54] D.L. Shaffer, N.Y. Yip, J. Gilron, M. Elimelech, Seawater desalination for agriculture by integrated forward and reverse osmosis: Improved product water quality for potentially less energy, J. Membr. Sci., 415-416 (2012) 1-8.

[55] C. Boo, M. Elimelech, S. Hong, Fouling control in a forward osmosis process integrating seawater desalination and wastewater reclamation, J. Membr. Sci., 444 (2013) 148-156.

[56] N.R.G. Walton, Electrical-Conductivity and Total Dissolved Solids - What Is Their Precise Relationship, Desalination, 72 (1989) 275-292.

[57] X. Jin, Q. She, X. Ang, C.Y. Tang, Removal of boron and arsenic by forward osmosis membrane: Influence of membrane orientation and organic fouling, J. Membr. Sci., 389 (2012) 182-187.